



# Study of tropospheric delay over Indian region from MODIS, NCEP/NCAR data and ground based water vapor measurements at Kolkata

Souvik Majumder, Saurabh Das, Animesh Maitra\*

*Institute of Radio Physics and Electronics, University of Calcutta, 92, A. P. C. Road, Kolkata 700009, India*

Received 19 March 2015; received in revised form 15 June 2015; accepted 16 June 2015

Available online 21 June 2015

## Abstract

A priori estimation of delays with error variance of atmospheric radio wave propagation is important for precise position estimation and integrity of the system like Global Positioning System (GPS). Tropospheric effects are less severe than the ionospheric counterpart, but behave in a complex manner, making it difficult to isolate them. In this present paper, a ground based radiometer has been utilized to study the characteristics of tropospheric delay and compared it with the MODIS satellite observations over Kolkata (22.57°N, 88.37°E). Results indicate a good agreement between radiometer and MODIS data except the monsoon months. A climatology of spatial and temporal variation of dry and wet tropospheric delay over the Indian subcontinent have also been estimated using MODIS data and NCEP–NCAR reanalysis data for 2008–2012. The spatial variations of dry delay over Indian region are observed to be in the range of 120–250 cm with limited seasonal variability. However, the wet delay varies from 20 cm in winter months to 45 cm during monsoon period in the coastal and central Indian region. Further analysis reveals that the contribution of wet delays in total delay is significant only along the Indo-Gangetic plain. This indicates that extra precaution is needed in handling tropospheric delay for this region due to fast varying nature of water vapor.

© 2015 COSPAR. Published by Elsevier Ltd. All rights reserved.

**Keywords:** Precise positioning; Global Positioning System (GPS); Precipitable water vapor (PWV); Tropospheric delay; Indian region

## 1. Introduction

The accuracy and integrity of precise point positioning (PPP) applications using GPS/GNSS depend primarily on propagation effects. The major source of uncertainty in GNSS is due to propagation effects on signals through the Earth's atmosphere (Pratt et al., 2003; Parkinson

et al., 1996). Ionosphere is the main source of the signal delay which can be handled using a dual frequency receiver. The remaining delay is mainly due to dry and wet component of the troposphere. The tropospheric dry delay is relatively stable for a particular temperature and pressure (Luo et al., 2013), but, the wet component is a highly variable quantity both in space and time (Brunner and Welsh, 1993).

The tropospheric delay becomes an important issue for PPP of the aircraft on the runway using GPS/GNSS during landing under severe weather conditions which requires an accuracy of less than 10 cm in real time. Tropospheric delay of the order of few decimeters can occur when the altitude difference between the aircraft and the reference

\* Corresponding author at: Institute of Radio Physics and Electronics, S. K. Mitra Centre for Research in Space Environment, University of Calcutta, 92, Acharya Prafulla Chandra Road, Kolkata 700009, India. Tel.: +91 33 2350 9116x45 (O); fax: +91 33 2351 5828.

E-mail addresses: [souvik1985.majum@gmail.com](mailto:souvik1985.majum@gmail.com) (S. Majumder), [das.saurabh01@gmail.com](mailto:das.saurabh01@gmail.com) (S. Das), [animesh.maitra@gmail.com](mailto:animesh.maitra@gmail.com) (A. Maitra).

station is about 0.5 km (Boon et al., 1997). Moreover, Very-Long-Baseline Interferometry (VLBI) is also very sensitive to this type of tropospheric delay (Pacione et al., 2002; Teke et al., 2013) since the multiple radio-telescope situated far away are used in this technique. Further, Interferometric Synthetic Aperture Radar (InSAR) used for generating images of surface deformation and elevation is also affected by the random variations of tropospheric delay (Xu et al., 2011; Massonnet et al., 1994; Rosen et al., 2000). The accuracy of measurements with InSAR images decreases up to 32% without using tropospheric correction (Xu et al., 2006). It is reported that a 20% change in humidity, which is the major source of tropospheric delay, may produce an error of 10 cm in the deformed products (Zebker et al., 1997).

To address this issue, externally estimated tropospheric delay using meteorological data or NWP are used (Cucurull et al., 2002; Tregoning and Herring, 2006). Accurate measurements of tropospheric parameters can also be made in differential mode for small baseline systems using either code or carrier base techniques. However, owing to the highly variable nature of tropospheric water vapor, it is very difficult to estimate the wet delay accurately due to the altitude difference (Kaplan and Hegarty, 2006) of the stations and from long baseline measurements (Blewitt, 1989). Further, carrier phase technique, which provides higher accuracy in PPP applications than the code based technique, is susceptible to integer ambiguity problems. The high variability of tropospheric water vapor can be a serious challenge in the case of integer ambiguity resolution of carrier phase data (Treuhaft and Lanyi, 1987; Blewitt, 1989; Bertiger et al., 2010; Zhang and Lachapelle, 2001). The correct estimation of *ZWD* values from the GPS data is also difficult due to multipath effects of low elevation satellite (Chen and Liu, 2014) and also due to use of various mapping functions, mostly developed using ray tracing of radiosonde data (Niell, 1996, 2001) and numerical weather prediction models or ECMWF data (Boehm and Schuh, 2004; Boehm et al., 2006).

There are several models and data products are currently available which deals with the tropospheric delay. The most notable of these data products on tropospheric delay is an IDS data product measured using GPS and GNSS post-processing at IGS stations (Byun and Bar-Sever, 2009; Dow et al., 2009). However, the applicability of such data products is limited since very few IGS stations are available, particularly over oceans and some part of the globe. Another important data set concerning the wet delay has been developed using DORIS technique (Bock et al., 2014).

The variability of PWV over Indian regions are directly related to the various factors including sea surface temperature of the Bay of Bengal and Arabian sea, land surface temperature over central India, monsoon rain and cyclonic activities (Singh et al., 2004). It was also reported that the PWV is highly variable in the Indo-Gangetic plain (Kumar et al., 2013). It is thus important to identify the regions

which will be most affected by wet tropospheric delay variations. In this paper, the variability of zenith tropospheric delay (*ZTD*), precipitable water vapor as well as tropospheric wet delay is studied over the location of Kolkata using a ground based radiometer and MODIS satellite observations. The study is then extended to cover the whole Indian region with long term MODIS observation (2008–2012) to identify the regions where serious errors in PPP applications can occur due to *ZWD* variability.

## 2. Data and methodology

A microwave radiometer (RPG-HATPRO) located at the Institute of Radio Physics and Electronics, University of Calcutta (22.57°N, 88.37°E), has been operated for ground based measurements. The radiometer measures the brightness temperature in real time basis with an accuracy of 0.5 K at 14 different frequencies in two frequency bands (22–31 GHz and 51–58 GHz). The radiometer generates *IWV* values using a quadratic regression method from brightness temperature at 22–31 GHz band with a time resolution of 3 s (Rose and Walber, 2010). Chakraborty et al. (2014) compared the same radiometer derived temperature and relative humidity profiles against the radiosonde observations which indicate a reasonably good performance of the instrument during the measurement period.

The ground meteorological data are collected using Paroscientific MET3A instrument at Kolkata. The pressure accuracy of this instrument is  $\pm 0.08$  hPa in the range of 620–1100 hPa, along with the temperature accuracy of  $\pm 0.1$  °C in the range of  $-50$  °C to  $+60$  °C.

In addition to radiometer data and meteorological data we have also used a ground based disdrometer for the observation of rain events during 2012–2014 in Kolkata. The disdrometer (Disdromet RD-80), is a Joss type drop size counter which has been used to obtain rain rate at the location. The dependency of water vapor on rainfall and temperature is also studied over Kolkata.

For the location of Kolkata, we have used local radiometer and meteorological data to estimate *ZWD* and *ZHD* during the year of 2012–2014. For rest of the Indian regions, temperature and pressure data are obtained from NCEP/NCAR reanalysis data product and *IWV* from MODIS instrument.

MODIS is the key instrument which is attached to the AQUA and TERRA satellite. This instrument can record data in 36 spectral bands ranging in wavelength from 0.4  $\mu\text{m}$  to 14.4  $\mu\text{m}$  and at various spatial resolutions. Several parameters like temperature of oceans and land, aerosol, water vapor content, cloud altitude in the lower atmosphere are obtained using these frequencies. We have used level-3 integrated water vapor (*IWV*) data obtained with AQUA satellite during the period 2008–2012 (<http://modis-atmos.gsfc.nasa.gov>) derived from the near infrared channels. The daily average values of the *IWV* obtained from Moderate Resolution Imaging Spectroradiometer (MODIS) and the radiometer are

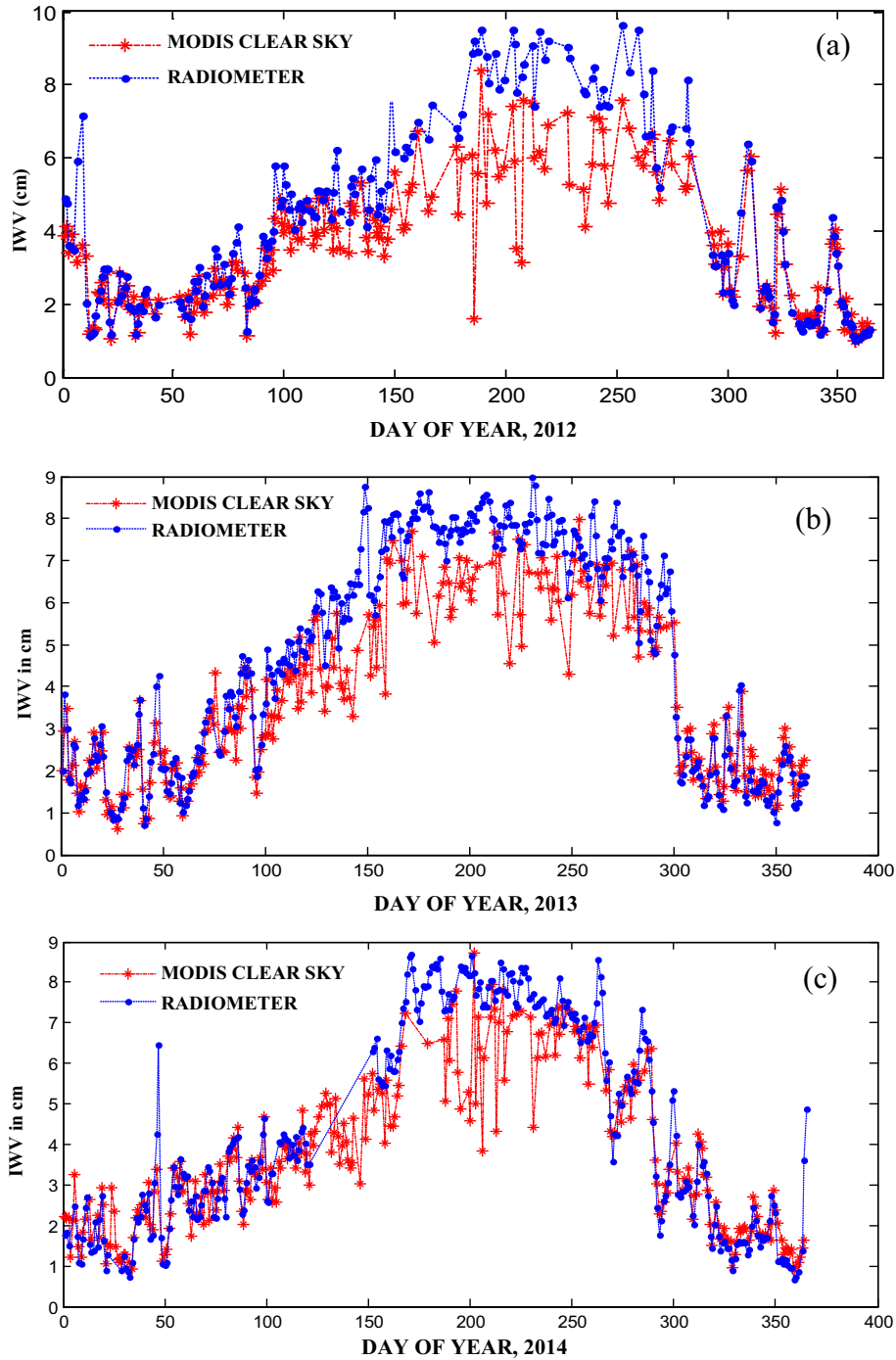


Fig. 1. Comparison of IWV data obtained from MODIS and radiometer for the year of (a) 2012, (b) 2013, (c) 2014.

compared for the period 2012–2014 over Kolkata. The gridded *IWV* data from MODIS on a daily basis for 2008–2012 have also been used and *ZWD* is calculated for each grid over Indian region.

The *ZWD* can be estimated from *IWV* using the following relation (Choy et al., 2013; Kumar et al., 2013),

$$ZWD = (IWV/\rho) \times K \quad (1)$$

where  $\rho$  is the density of the water  $\text{kg/m}^3$  and  $K$  is a dimensionless quantity given by

$$K = 10^{-6} \left( \frac{k_3}{T_m} + k'_2 \right) \cdot \rho \cdot R_V \quad (2)$$

where  $R_V$  is the water vapor gas constant,  $T_m$  is weighed temperature of the atmosphere and,  $k'_2$  and  $k_3$  are constants.

*ZHD* for the same duration is also estimated from gridded NCEP–NCAR data. The NCEP–NCAR reanalysis dataset which is a combined product from National Centre for Environmental Prediction (NCEP) and the

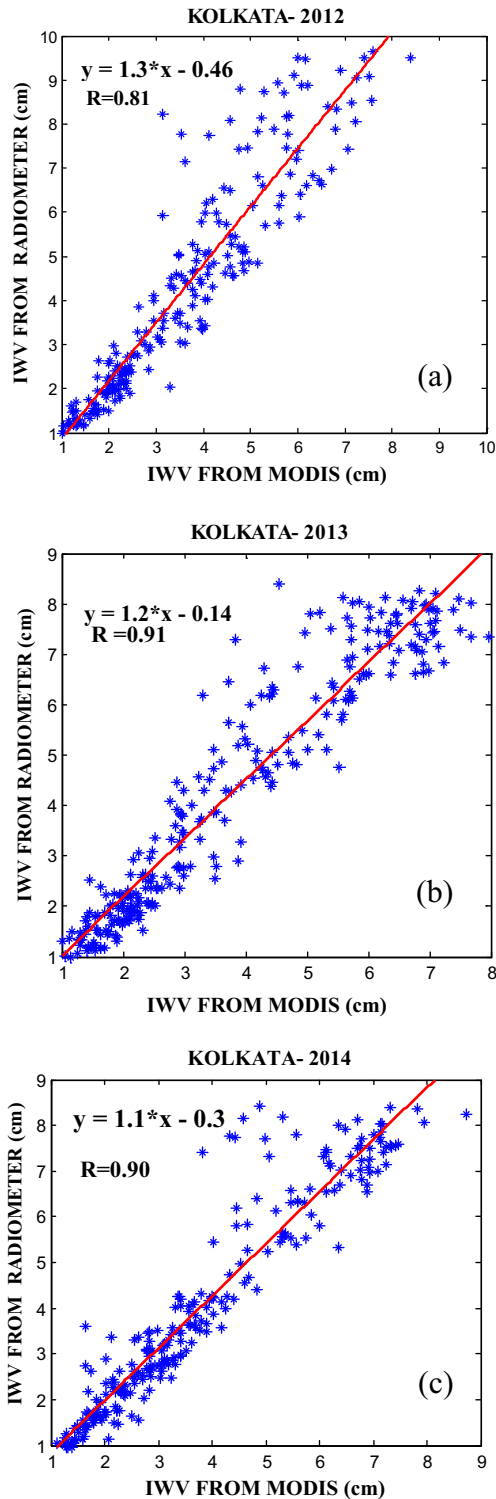


Fig. 2. Correlation of IWV data obtained from MODIS and radiometer for the year of (a) 2012, (b) 2013, (c) 2014.

National Centre for Atmospheric Research (NCAR) is utilized for temperature and pressure measurement over  $2.5^\circ \times 2.5^\circ$  grids for the period 2008–2012. It was reported that temperature and barometric measurements for low altitude stations show a good agreement with that provided in NCEP/NCAR data (Quinn and Herring, 1996).

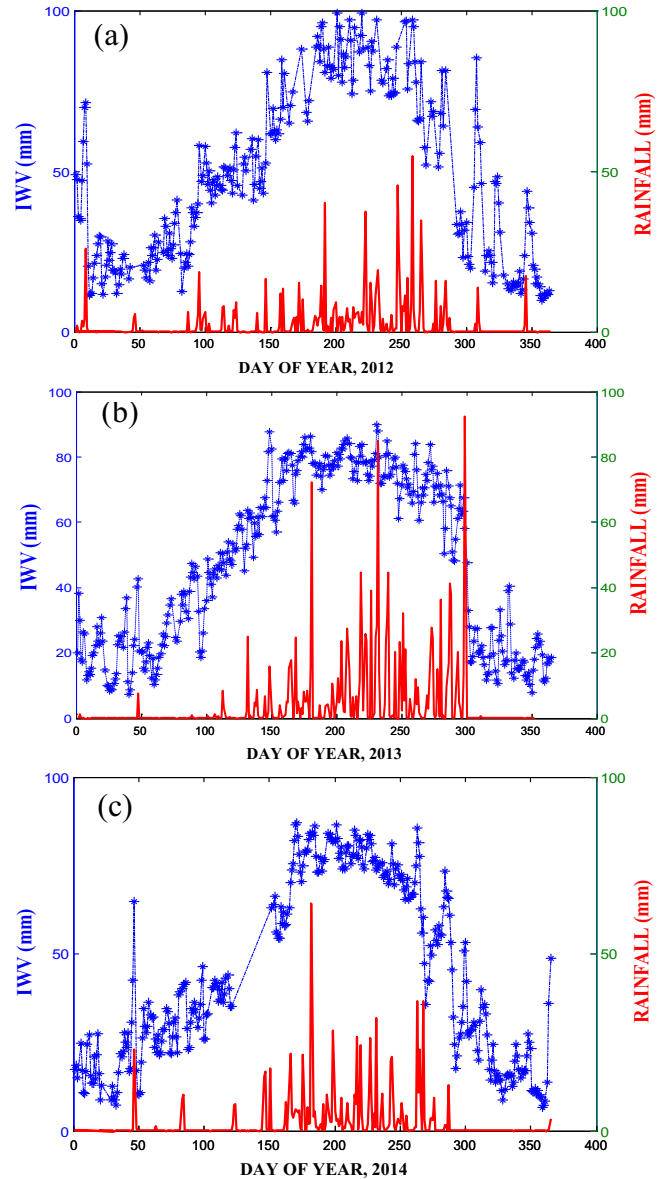


Fig. 3. Variation of ground observed rainfall with IWV over Kolkata for years (a) 2012, (b) 2013, (c) 2014.

The hydrostatic delay which is a major contributor of total GPS signal delay in the troposphere can be estimated using various models. For the present study, we have used Hopfield model (Das et al., 2014). According to this model ZHD can be expressed as,

$$ZHD = 1.552(h - H) \frac{P}{T} \tag{3}$$

where  $h = 40.082 + 0.14898(T - 273.16)$ ,  $H$  is the height of station above sea level (km),  $T$  is the surface temperature (K) and  $P$  is surface pressure (hPa).

To identify the regions which are most susceptible to tropospheric delay variation, contribution of ZWD in the total tropospheric delay is estimated over India for different months and, the range and the standard deviation of ZWD for each grid were estimated.

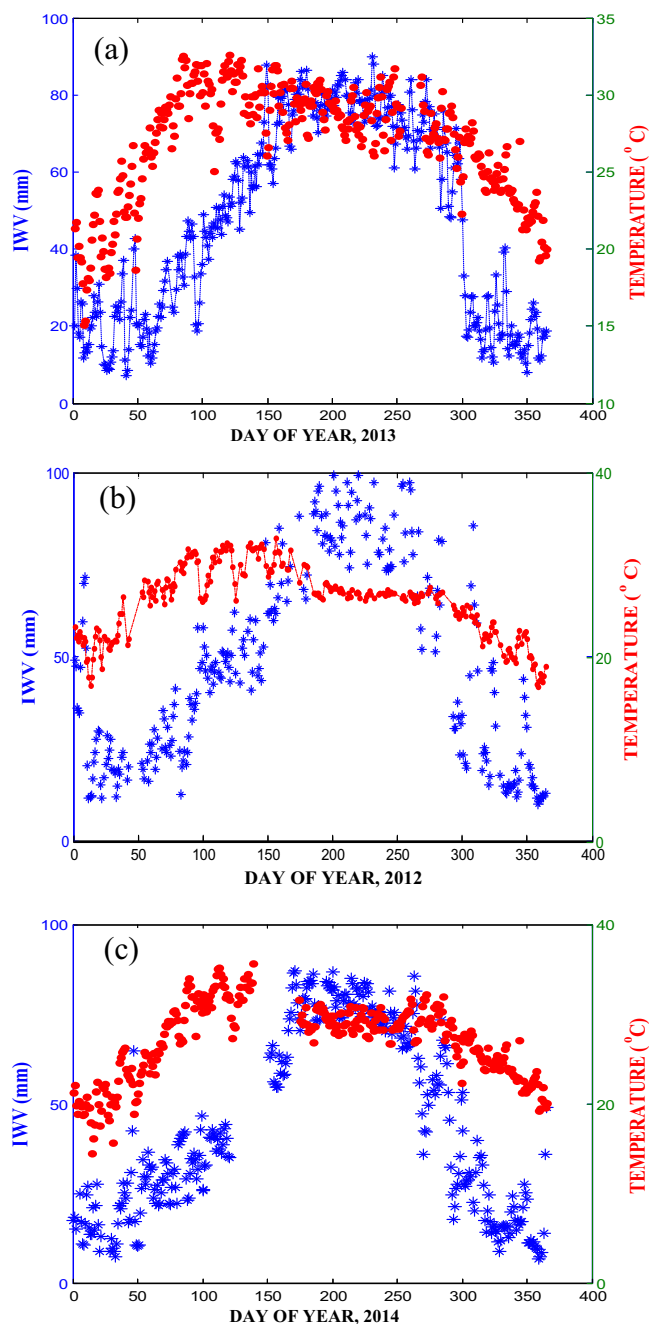


Fig. 4. Variation of surface temperature with I WV over Kolkata for years (a) 2012, (b) 2013, (c) 2014.

### 3. Results and discussions

Since measured tropospheric delay data over Indian region are sparse, satellite based measurements of water vapor are used to estimate the tropospheric delay and its variability over Indian region. The satellite observations such as Terra-MODIS, SSM/I, AIRS etc. are previously used by various researchers for water vapor study over the Indian region (Prasad et al., 2009; Singh et al., 2010; Kumar et al., 2013) which are in good agreement with ground observations. In the present study, we use the Aqua-MODIS data.

#### 3.1. Comparison of MODIS and ground based radiometer data

The clear-sky I WV data from AQUA-MODIS is compared to the I WV data of radiometer obtained at Kolkata during the year 2012–2014 as shown in Fig. 1. A good matching between these two sets of data can be seen from the Fig. 1(a–c), except for the days ranging from  $\sim 150$  to  $\sim 250$  of the year. This period actually represents the rainy season during which radiometer measurements are less accurate. Thus the comparison between the MODIS and ground radiometer is only meaningful in non-rainy period, which indicates satisfactory performance of MODIS over this region.

In Fig. 2(a–c), the scatter plot between the daily I WV values obtained from the local radiometer and MODIS is shown for the Kolkata region during 2012–2014. The figures also indicate a good correlation between the two instruments for all three years with correlation coefficient values of  $\sim 0.9$ .

#### 3.2. Variability of water vapor with rainfall and temperature for Kolkata region

I WV is dependent on surface temperature and rainfall (Bretherton et al., 2004). In Fig. 3, the variation of I WV and rainfall for the Kolkata region during 2012–2014 is shown.

Since rainfall over Indian region is mostly governed by monsoon circulation, we calculated the correlation values between the daily I WV values and the amount of rainfall during the year 2012–2014 on a seasonal basis. The value of correlation coefficient is found to be  $\sim 0.5$  during pre-monsoon (March–May) and  $\sim 0.45$  during monsoon (June–September) and postmonsoon (October–January) period.

In Fig. 4, the variation of I WV with temperature is shown for the Kolkata region during 2012–14.

During years 2012–2014, correlation coefficient values are observed to be in the range 0.4–0.6 during the premonsoon period, whereas higher values of correlation coefficient around  $\sim 0.65$  are obtained during the post monsoon period. However, during monsoon season, values of correlation coefficient are obtained in the range of  $-0.5$  to  $-0.8$ , indicating that an increase of I WV causes more rainfall cooling down the ground temperature.

#### 3.3. Seasonal behavior of ZHD and ZWD over Kolkata

In Fig. 5, the seasonal behavior of ZHD and ZWD are shown for Kolkata during the year 2012–2014. The ZHD is estimated from the ground temperature and pressure data from NCEP–NCAR reanalysis data. Similarly the values of ZWD are estimated from the I WV data provided by MODIS. The monthly average value of ZHD and ZWD show that the variation of ZHD is small, ranging from

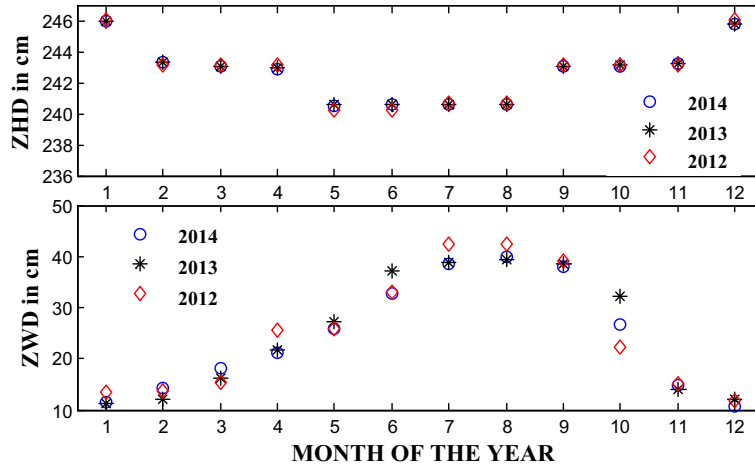


Fig. 5. Monthly values of ZHD and ZWD over Kolkata during various months of the year, 2012–2014.

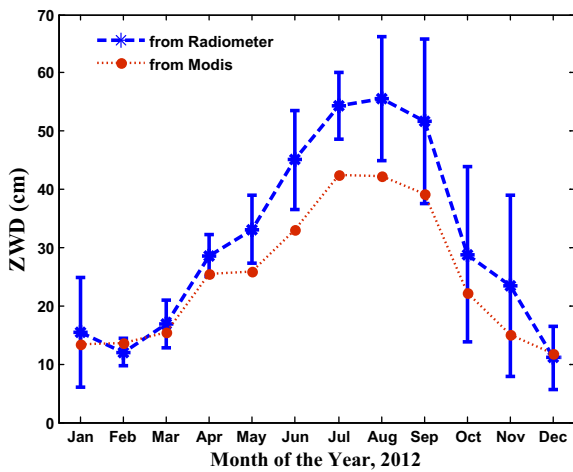


Fig. 6. Monthly variation of ZWD over the Kolkata region during the year of 2012 as obtained from radiometer observation and MODIS data.

240 cm to 250 cm, whereas the monthly variation of *ZWD* is large ranging from 10 cm to 50 cm.

The possible reason for relatively small variation in *ZHD* is due to the fact that *ZHD* does not change significantly with temperature and pressure. For example, if  $H = 1$  km,  $P = 1000$  mbar, the variation of *ZHD* will be between 227.7 and 228.5 cm (i.e.  $\sim 1$  cm) for a temperature change of 270–350 K.

However, the seasonal variability of water vapor is found to be significant. The values of *ZWD* obtained from MODIS are compared with that derived from the local meteorological sensor and radiometer and the comparison is shown in Fig. 6 for the year of 2012. Two curves show a similar pattern except for the monsoon months, May–September 2012, as the radiometer does not yield accurate data under rainy conditions (Das et al., 2014).

### 3.4. Variability of tropospheric delay over India

#### 3.4.1. Variations of ZHD

To check whether the seasonal variations of *ZHD* are significant over Indian region, mean *ZHD* is estimated for each grid on a monthly basis for the year 2008–2012. Fig. 7 shows the average value of *ZHD* during the month of January for the years 2008–2012. A similar pattern is obtained for the other months of 2008–2012, though not shown here as the seasonal variations of *ZHD* is insignificant over Indian region. It is to be noted that the maximum seasonal changes of temperature of about 45 K are observed in the northern part of India, whereas for the rest part of Indian region, the seasonal temperature change is within 25 K. Also, the seasonal variations of pressure are within 20 mbar in this region. As a result, the whole Indian region does not experience much seasonal variation of *ZHD* values. Fig. 7 also shows that *ZHD* values may differ from one region to another. The contour plot in the diagram shows that the maximum average value of *ZHD* reached up to 250 cm over southern India. The coastal part of western, eastern and southern India shows

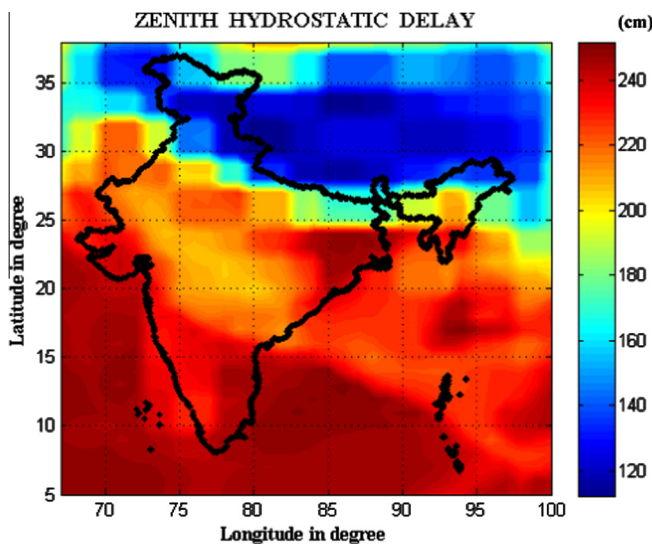


Fig. 7. Contour plot of ZHD at various latitude and longitude over the whole Indian region (averaged for 2008–2012).

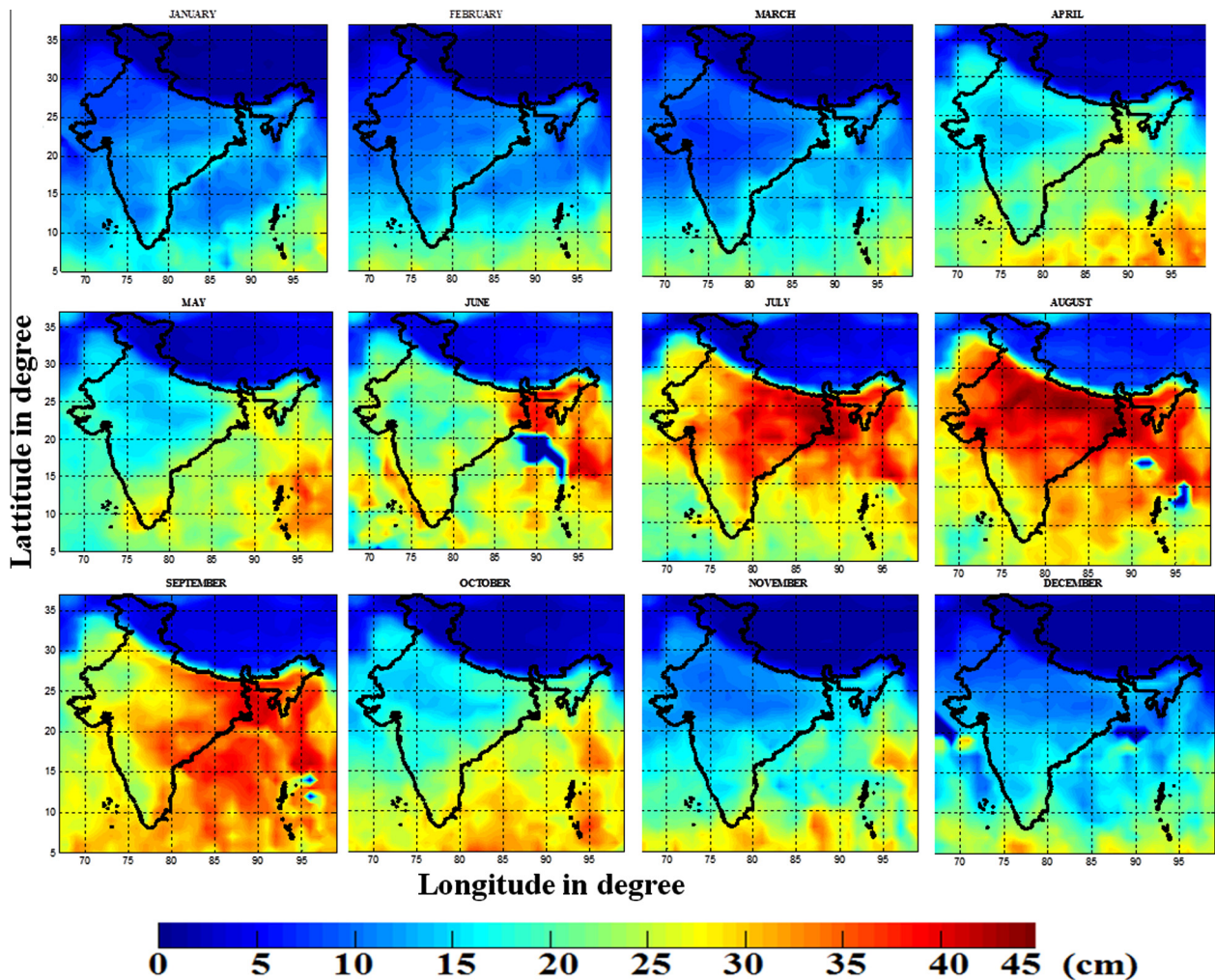


Fig. 8. Contour plots of ZWD during different months over the whole Indian region (averaged for 2008–2012).

the values of  $ZHD$  ranging from 220 cm to 250 cm due to higher temperature and pressure compared to the rest part. The amount of  $ZHD$  in the central Indian region is intermediate between 200 cm and 220 cm, whereas, it ranges from 160 cm to 200 cm in the transitional plains covering the Middle Gangetic Plain.

Northern part of India apparently suffers less dry delay ranging from 120 to 150 cm. A large portion of North and North-Eastern region is situated on the Himalayan mountain range where the pressure and temperature are low which is rather an extreme weather condition. However, in Fig. 7, an overall low value of  $ZHD$  has been obtained for these regions obtained from NCEP/NCAR data which has less accuracy in high altitude locations (Quinn and Herring, 1996).

#### 3.4.2. Variations of ZWD

The variation of  $ZWD$  on a monthly basis in the Indian region is shown in Fig. 8. The monthly mean value of  $IWW$  data as obtained from MODIS are converted into  $ZWD$  values using the previously mentioned Eqs. (1)–(3) and are depicted in Fig. 8 in the form of contours.

The value of  $ZWD$  depends much on the capacity of the atmosphere to hold water vapor (without precipitating) as well as the supply of water vapor which is highly dependent on the surface temperature and rainfall.

Indian monsoon is categorized into two types. The South-west monsoon, which produces large amounts of rainfall in the Indian subcontinent during June–September blows from the southwest during the warmer months, while, the north-east monsoon reverses its direction to blow from the north-east during the cooler months of the year causing rainfall mostly over the east coast of the southern peninsula (Gadgil, 2003).

Fig. 8 indicates that in the south coastal region, the minimum value of  $ZWD$  is 20 cm, whereas for the high altitude Himalayan and Tibetan region (i.e., Srinagar, Shimla, Sikkim), the value of  $ZWD$  seldom increases above 15 cm. In the undulated terrain like the Himalayan sites or Tibetan plateau, amount of  $ZWD$  is significantly small throughout the year, the maximum value being 10–12 cm. This is due to lack of rainfall in those regions which is not noticed for the other Indian regions. The monthly mean values of  $ZWD$  vary in the range of 25–45 cm in

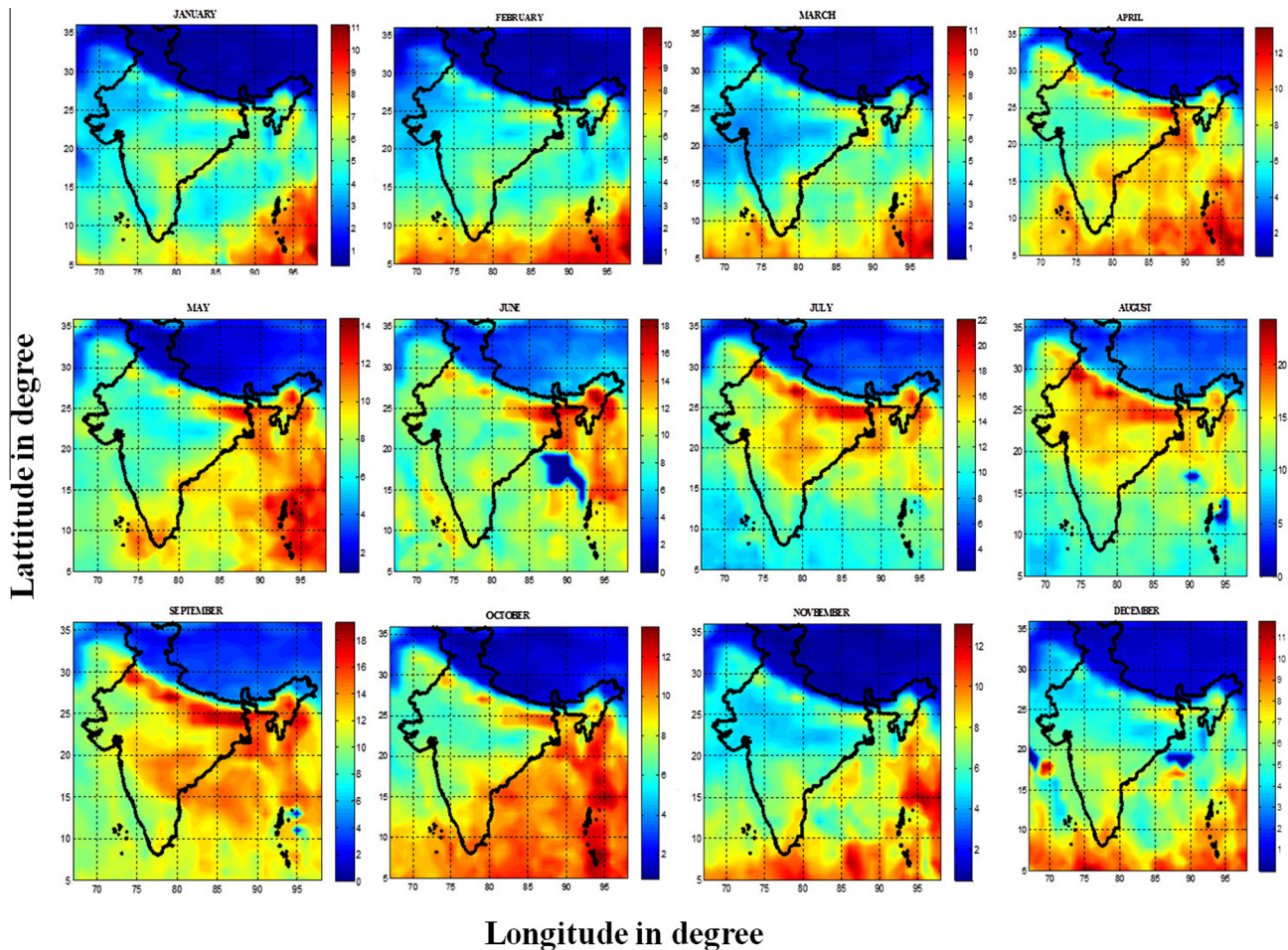


Fig. 9. Contour plot of percentage of ZWD over total tropospheric delay at various latitude and longitude over the whole Indian region (averaged for 2008–2012).

the coastal region and the southern part of India. But, the variation becomes 15–35 cm for the central portion of India during the year. The value of mean ZWD also varies from 10 cm to 25 cm in dry season and 20–35 cm in the humid condition of the Eastern part. This difference in the monthly variation of ZWD at these stations is mainly caused by the large variability in atmospheric water vapor content.

During the months of December–February (winter season) ZWD is relatively lower over the whole Indian region. But, as we approach the Indian summer monsoon season, ZWD increases with the arrival of water vapor. During the months of May–June, ZWD shows a higher value in the coastal part compared to inland parts of India because of the supply of water vapor from the sea. In the monsoon months (i.e. June, July, August), water vapor is spread out in the whole eastern, central, western and southern portion of India due to favorable wind condition and ZWD consequently increases reaching up to 40–45 cm. In the post monsoon months, the value of ZWD gradually decreases in the eastern, central and western India.

The monthly variation of ZWD is small for the tropical coastal station compared to the other stations of the

central, eastern and western India. It is also noticeable, that in the southern coastal part of India, the value of ZWD is quite moderate and consistent (ranging from 25 cm to 35 cm) during the whole year. This can be explained in terms of the higher water vapor content in those regions which is due to the presence of by southwest and northeast monsoon and comparatively high temperature throughout the year. Not only that, in the winter period the absolute values of ZWD of the southern coastal stations are higher than the other inland stations of India as the temperature is much higher of these regions than that of the higher latitude station during the whole year. As a result, the atmosphere can hold relatively more water vapor in the coastal area, and southern part of India (Singh et al., 2010). For the same reason, the value of ZWD of the whole Indian region is higher during July and August as the air temperature is high at that period.

### 3.5. Contribution of ZWD variation in total tropospheric delay

The contribution of ZWD to the total tropospheric delay is depicted in Fig. 9. In the winter season, the

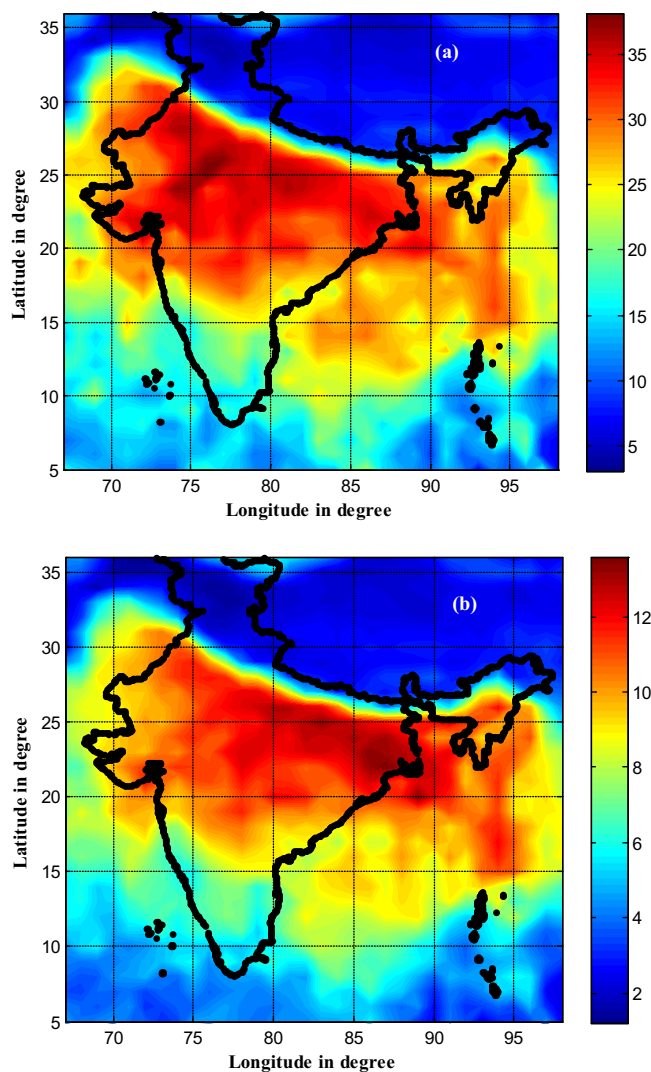


Fig. 10. Contour plot of (a) range of  $ZWD$  and (b) standard deviation of  $ZWD$  at various latitude and longitude over the whole Indian region (averaged for 2008–2012).

proportion of  $ZWD$  in the total tropospheric delay reaches up to a maximum value of 11% only and increases to 22% in the monsoon period. The contribution of  $ZWD$  to the total tropospheric delay in the Himalayan and terrain part of India shows a small variation throughout the whole year. It has been noticed that in the rainy season, contribution of  $ZWD$  to the total tropospheric delay is large in the central east India and central west India compared to the other location. In the coastal Indian zone and southern India,  $ZWD$  contributes moderately throughout the whole year (ranging from 5% to 10%).

To understand the significance of this variation, the range (i.e. the difference between maximum and minimum value of  $ZWD$ ) and the standard deviation of the  $ZWD$  for each grid are shown in Fig. 10. It can be seen from Fig. 10(a and b), that the significant variability of  $ZWD$  is observed only in the region from latitude of  $20^{\circ}\text{N}$  to  $25^{\circ}\text{N}$  and longitude of  $70^{\circ}\text{E}$  to  $90^{\circ}\text{E}$ . However, the standard deviation indicates that, the significant variability is

mainly concentrated in the region from latitude of  $20^{\circ}\text{N}$  to  $25^{\circ}\text{N}$  and longitude of  $77^{\circ}\text{E}$  to  $87^{\circ}\text{E}$ . The reason behind such observation is that although the seasonal variation is large over the longitude of  $70^{\circ}\text{E}$  to  $90^{\circ}\text{E}$  but, the fluctuations of  $ZWD$  are concentrated mainly in the longitude of  $77^{\circ}\text{E}$  to  $87^{\circ}\text{E}$  due to high occurrence of random weather phenomena. More precisely the greater standard deviation of  $ZWD$  is observed along the Indo-Gangetic plain. On the other hand, the Southern peninsular region has high  $ZWD$  value during monsoon and post monsoon months, though the variation is relatively less. Singh et al. (2010) also reported similar observation of total PWV using SSM/I data. Since, the precise positioning applications, requires a priori information of  $ZWD$ , any sudden fluctuation of water vapor content can induce significant error. Our analysis shows that the error due to  $ZWD$  variation can be significantly high over the region covered by the latitude range from  $20^{\circ}\text{N}$  to  $25^{\circ}\text{N}$  and the longitude range from  $77^{\circ}\text{E}$  to  $87^{\circ}\text{E}$  and not over the entire Indian subcontinent.

#### 4. Conclusion

The tropospheric delay introduces sensitive errors in the case of precise positioning applications including aircraft landing. It is also an important issue in InSAR data processing and VLBI measurements. The water vapor variability is the major source of uncertainty in total tropospheric delay. A study of the seasonal and spatial variability of  $ZWD$  and  $ZHD$  over the Indian region has been presented using NCEP–NCAR reanalysis data set and MODIS observations. A climatological study on the relationship among water vapor, rainfall and temperature over the location of Kolkata has also been made.

The wet tropospheric delay ( $ZWD$ ) exhibits a seasonal variation, whereas the dry tropospheric delay ( $ZHD$ ) does not show such seasonal trend. The total delay is higher in the monsoon months in comparison to winter time due to this seasonal effect of  $ZWD$ . It is also observed that the spatial variability of  $ZHD$  over Indian region varies from 120 cm at Northern Indian region to 250 cm at the south and central east part of India. The wet delay varies in the Indian region between 5 cm and 45 cm depending upon season and location. The contribution of  $ZWD$  in total tropospheric delay is highest during the monsoon months (June–September) for the Indo-Gangetic plain, central, east and southern coastal part of India. However, the temporal variability is most prominent only in the Indo-Gangetic plain, the region between  $20^{\circ}\text{N}$  to  $25^{\circ}\text{N}$  and longitude of  $77^{\circ}\text{E}$  to  $87^{\circ}\text{E}$ . The result indicates that these regions are more vulnerable to positioning error due to sudden change in tropospheric delay and extra precaution is required for processing of relevant data of these regions.

#### Acknowledgements

Financial support provided by (1) “Indian Space Research Organization” (ISRO) under the projects

“Space Science Promotion Scheme” and (2) “Technical Education Quality Improvement Programme” (TEQIP) Phase-II” are thankfully acknowledged.

## References

- Bertiger, W., Desai, S.D., Haines, B., Harvey, N., Moore, A.W., Owen, S., Weiss, J.P., 2010. Single receiver phase ambiguity resolution with GPS data. *J. Geodesy* 84 (5), 327–337.
- Blewitt, G., 1989. Carrier phase ambiguity resolution for the Global Positioning System applied to geodetic baselines up to 2000 km. *J. Geophys. Res.* 94 (B8), 10187–10203.
- Bock, O., Willis, P., Wang, J., Mears, C., 2014. A high-quality, homogenized, global, long-term (1993–2008) DORIS precipitable water data set for climate monitoring and model verification. *J. Geophys. Res. Atmos.* 119 (12), 7209–7230.
- Boehm, J., Schuh, H., 2004. Vienna mapping functions in VLBI analyses. *Geophys. Res. Lett.* 31 (1). Article Number: L01603.
- Boehm, J., Niell, A., Tregoning, P., Schuh, H., 2006. Global Mapping Function (GMF): a new empirical mapping function based on numerical weather model data. *Geophys. Res. Lett.* 33 (7). Article Number: L07304.
- Boon, F.J.G., de Jonge, P.J., Tiberius, C.C.J.M., 1997. Precise aircraft positioning by fast ambiguity resolution using improved troposphere modelling. In: Proc of the 10th International Technical Meeting of the Satellite Division of The Institute of Navigation (ION GPS 1997), 1877–1884.
- Bretherton, C.S., Peters, M.E., Back, L.E., 2004. Relationships between water vapor path and precipitation over the tropical oceans. *J. Climate* 17, 1517–1528.
- Brunner, F.K., Welsh, W.M., 1993. Effects of the troposphere on GPS Measurements. *GPS World* 4 (1), 42–51.
- Byun, S.H., Bar-Sever, Y.E., 2009. A new type of troposphere zenith path delay product of the international GNSS service. *J. Geodesy* 83 (3–4), 367–373.
- Chakraborty, R., Das, S., Jana, S., Maitra, A., 2014. Nowcasting of rain events using multi-frequency radiometric observations. *J. Hydrol.* 513, 467–474.
- Chen, B., Liu, Z., 2014. Voxel-optimized regional water vapor tomography and comparison with radiosonde and numerical weather model. *J. Geodesy*. <http://dx.doi.org/10.1007/s00190-014-0715-y>.
- Choy, S., Wang, C., Zhang, K., Kuleshov, Y., 2013. GPS sensing of precipitable water vapor during the March 2010 Melbourne storm. *Adv. Space Res.* 52 (9), 1688–1699.
- Cucurull, L., Sedo, P., Behrend, D., Cardellach, E., Rius, A., 2002. Integrating NWP products into the analysis of GPS observables. *Phys. Chem. Earth (A)* 27, 377–383.
- Das, S., Majumder, S., Chakraborty, R., Maitra, A., 2014. A simplistic approach for water vapor sensing using a stand alone GPS receiver. *IET Radar Sonar Navig.* <http://dx.doi.org/10.1049/iet-rsn.2013.0312>.
- Dow, J.M., Neilan, R.E., Rizos, C., 2009. The International GNSS service in a changing landscape of global navigation satellite systems. *J. Geodesy* 83 (3–4), 191–198.
- Gadgil, S., 2003. The Indian monsoon and its variability. *Annu. Rev. Earth Planet. Sci.* 31, 429–467.
- Kaplan, E.D., Hegarty, C.J., 2006. *Understanding GPS: Principles and Applications*, second ed. Artech House.
- Kumar, S., Singh, A.K., Prasad, A.K., Singh, R.P., 2013. Variability of GPS derived water vapor and comparison with MODIS data over the Indo-Gangetic plains. *Phys. Chem. Earth* 55–57 (2013), 11–18.
- Luo, X., Heck, B., Awange, J.L., 2013. Improving the estimation of zenith dry tropospheric delays using regional surface meteorological data. *Adv. Space Res.* 52 (12), 2204–2214.
- Massonnet, D., Feigl, K., Rossi, M., Adragna, F., 1994. Radar interferometric mapping of deformation in the year after the Landers earthquake. *Nature* 369, 227–230.
- Niell, A.E., 1996. Global mapping functions for the atmosphere delay at radio wavelengths. *J. Geophys. Res.* 101, 3227–3246.
- Niell, A.E., 2001. Preliminary evaluation of atmospheric mapping functions based on numerical weather models. *Phys. Chem. Earth* 26, 475–480.
- Pacione, R., Fionda, E., Ferrara, R., Lanotte, R., Sciarretta, C., Vespe, F., 2002. Comparison of atmospheric parameters derived from GPS, VLBI and a ground-based microwave radiometer in Italy. *Phys. Chem. Earth* 27, 309–316.
- Parkinson, B.W., Enge, P.K., Spilker, J.J., 1996. *Differential GPS in Global Positioning System: theory and applications*. Am. Inst. Aeronaut. Astronaut. II, 3–115, Washington, DC.
- Prasad, A.K., Singh, R.P., 2009. Validation of MODIS Terra, AIRS, NCEP/DOE AMIP-II Reanalysis-2, and AERONET Sun photometer derived integrated precipitable water vapor using ground-based GPS receivers over India. *J. Geophys. Res.* 114. Article Number: D05107.
- Pratt, T., Bostian, C., Allnutt, J., 2003. *Satellite Communication*, second ed. Wiley, New York.
- Quinn, K.J., Herring, T.A., 1996. GPS Atmospheric Water Vapor Measurements without the Use of Local Barometers. AGU Fall Meet 1996, Poster G12A-06.
- Rose, T., Walber, A., 2010. Radiometer Physics GmbH, RPG Radiometer Physics GmbH, Birkenmaarastraße 10-53340 Meckenheim/Germany.
- Rosen, P.A., Hensley, S., Joughin, I.R., Li, F.K., Madsen, S.N., Rodriguez, E., Goldstein, R.M., 2000. Synthetic aperture radar interferometry. *Proc. IEEE* 88 (3), 333–382.
- Singh, R.P., Dey, S., Sahoo, A.K., Kafatos, M., 2004. Retrieval of water vapor using SSM/I and its relation with the onset of the monsoon. *Ann. Geophys.* 22, 3079–3083.
- Singh, R.P., Mishra, N.C., Verma, A., Ramaprasad, J., 2010. Total precipitable water over Arabian and Bay of Bengal using SSM/I data. *Int. J. Remote Sens.* 21 (12), 2497–2503.
- Teke, K., Nilsson, T., Böhm, J., Hobiger, T., Steigenberger, P., García-Espada, S., Haas, R., Willis, P., 2013. Troposphere delays from space geodetic techniques, water vapor radiometers, and numerical weather models over a series of continuous VLBI campaigns. *J. Geodesy* 87, 981–1001.
- Tregoning, P., Herring, T.A., 2006. Impact of a priori zenith hydrostatic delay errors on GPS estimates of station heights and zenith total delays. *Geophys. Res. Lett.* 33, L23303. <http://dx.doi.org/10.1029/2006GL027706>.
- Treuhaft, R.N., Lanyi, G.E., 1987. The effect of the dynamic wet troposphere on radio interferometric measurements. *Radio Sci.* 22 (2), 251–265.
- Xu, C., Wang, H., Ge, L., Yonezawa, C., Cheng, P., 2006. InSAR tropospheric delay mitigation by GPS observations: a case study in Tokyo area. *J. Atmos. Sol. Terr. Phys.* 68 (6), 629–638.
- Xu, W.B., Li, Z.W., Ding, X.L., Zhu, J.J., 2011. Interpolating atmospheric water vapor delay by incorporating terrain elevation information. *J. Geodesy* 85 (9), 555–564.
- Zebker, H.A., Rosen, P.A., Hensley, S., 1997. Atmospheric effects in interferometric synthetic aperture radar surface deformation and topographic maps. *J. Geophys. Res.* 102 (B4), 7547–7563.
- Zhang, J., Lachapelle, G., 2001. Precise estimation of residual tropospheric delays using a regional GPS network for real-time kinematic applications. *J. Geodesy* 75, 255–266.